



Multi-walled carbon nanotubes/polypyrrole nanocomposite, synthesized through an eco-friendly route, as a prospective drug delivery system

P. Saheeda¹ · Y. M. Thasneem² · K. Sabira¹ · M. Dhaneesha³ · N. K. Sulfikkarali⁴ · S. Jayalekshmi¹

Received: 11 November 2021 / Revised: 30 March 2022 / Accepted: 13 May 2022 /
Published online: 29 May 2022

© The Author(s), under exclusive licence to Springer-Verlag GmbH Germany, part of Springer Nature 2022

Abstract

A smart drug delivery system involving the nanocomposite of multi-walled carbon nanotubes (MWCNTs) and polypyrrole (PPy) loaded with the drug, curcumin has been developed through ecofriendly routes. The nanocomposite exhibits pH dependent and sustained drug release over a prolonged period. Functionalization of MWCNTs via lemon fruit extract provides water dispersible MWCNTs, which can be used as the drug carrier with reduced toxicity and enhanced biocompatibility. The inner void spaces of functionalized MWCNTs are used for storing drug which results in enhanced curcumin encapsulation of about 89%. Morphological, structural and chemical characterization of the developed nanocomposite has been carried out using field emission scanning electron microscopy (FESEM), transmission electron microscopy (TEM), X-ray diffraction (XRD) and Fourier Transform infrared (FTIR) spectroscopy techniques. Dynamic light scattering experiment reveals that the size and zeta potential of drug loaded nanocomposite lie within the ideal range of 172–194 nm and 18.4 mV, respectively. Ease of cellular uptake and chemotherapeutic potency of curcumin loaded nanocomposite are confirmed through fluorescence imaging under in vitro conditions. Finally, the safety profile of acid functionalized MWCNTs/PPy nanocomposite is endorsed by the cytocompatibility analysis, carried out using SRB assay. Altogether, the nanocomposite developed in the present work through green chemistry routes, is one step ahead as a versatile carrier to deliver hydrophobic drugs like curcumin, and offers great promise in drug delivery applications.

Keywords Drug delivery · Polymerization · Encapsulation efficiency · Zeta potential · Cell viability · Cytotoxicity

✉ S. Jayalekshmi
jayalekshmi@cusat.ac.in

Extended author information available on the last page of the article

Introduction

Nanoparticles (NPs)-based drug delivery systems (DDSs) are gaining intense research interest in the global scenario because they can overcome many of the limitations of traditional drug delivery systems such as nonspecific targeting, lack of solubility and inability to enter the core of the tumor sites [1–4]. Recent research efforts in nano-biotechnology are mainly focusing on developing efficient drug delivery systems using novel materials at the molecular level so that they can interact with the living cells of the body with the added benefits of precise and timely release of drugs. Nanosized drug carriers have high surface-to-volume ratio, which provides high drug loading efficiency and drugs can be transported to any part of the body without causing any blockage and delivered at the required destinations [5–7]. Nanoparticles can be tailored to get direct access of diseased cells selectively which makes accurate delivery of drugs feasible, simultaneously avoiding interaction with healthy cells [8]. Conventionally most of the drugs have been formulated to be delivered through oral and injection routes, with the disadvantage of systemic side effects due to their nonspecific bio-distribution and uncontrollable drug release characteristics. These difficulties are overcome by developing smart DDSs which can effectively reduce the dosage frequency, while maintaining the drug concentration in targeted organs for a sufficiently longer period of time and thus ensuring safe delivery of drugs to specific areas of the body [9, 10]. The most appealing thing about NPs-based DDSs is that they can facilitate the delivery of hydrophobic and poorly bioavailable drugs, and can protect drugs from premature degradation before they reach the target [11, 12]. The main challenge in the development of appropriate drug delivery systems is that they should ensure localized and controlled release of drugs with minimal side effects and increased therapeutic efficacy.

Carbon nanotubes (CNTs), are one dimensional cylindrical macromolecules consisting of hexagonal arrangement of sp^2 hybridized carbon atoms [13, 14]. Unique combination of their structural, electronic, and optical properties has opened new frontiers in the field of nanobiotechnology, offering host of opportunities in the development of new generation nanoscale tools and devices for biomedical applications [15–17]. Functionalized CNTs can effectively cross biological barriers which facilitates easier cellular uptake and their high drug loading capacity render them useful for nanostructure mediated therapeutic and diagnostic applications [18, 19]. Exceptionally high drug loading capacity and the possibility for incorporating therapeutic moieties on their surfaces or inner cavities have been exploited in the design of novel drug carrier systems [20]. Recently CNTs have gained increasing acceptance in biomedical research as efficient drug delivery vehicles over other nanocarriers owing to the possibility of utilizing their inner cavities as store places of drugs [21]. Hollow cylindrical configuration of CNTs has the advantage that their inner voids can be loaded with large amounts of drug molecules and can be carried and delivered to different cell sites. In addition, this strategy allows the protection of unstable drugs during their transportation eliminating the degradation of drugs before reaching the delivery sites.

Carbon nanotubes (CNTs) assisted drug delivery systems require deliberate cutting of CNTs into nanoscale fragments with their end caps removed, so that inner volumes of the tubes become accessible for loading drugs. Functionalization using appropriate strategy can bring about the desired structural changes, ensuring hydrophilicity and biocompatibility to the CNTs so that the nanotubes can be filled with drug containing solutions through sonication [21]. Hollow structure of MWCNTs with appreciable inner diameter has become an ideal geometry for drug transport and delivery in physiological systems.

Polypyrrole (PPy) is a light weight organic polymer formed by polymerization of monomer pyrrole. It is an inherently conducting polymer, endowed with an extensive, conjugated π electron system on the polymer backbone [22]. Biocompatibility, nontoxicity and in vivo stability of polypyrrole make it a promising material in biomedical applications [23]. Spongy texture of PPy is suitable for trapping nanoparticles and the stabilization of nanoparticles within the polymer matrix can also be ensured [24]. Though there are reports on DDSs based on electrical stimulation of PPy, only very few reports are available on the pH dependent drug release behavior of PPy [25, 26]. Wang and co-workers have studied pH-sensitive release of anti-tumor agent, doxorubicin (DOX) from hollow PPy nanocapsules, highlighting the release of more than half of the encapsulated drug within 15 h at a pH of 4.5 [27].

Generally, polypyrrole is synthesized via chemical oxidative polymerization of pyrrole in the presence of strong oxidizing agents such as ferric chloride (FeCl_3) and ammonium peroxodisulphate ($(\text{NH}_4)_2\text{S}_2\text{O}_8$) which leaves traces of toxic elements within the synthesized polymer and affects adversely its suitability for bio-related applications [28]. Use of hydrogen peroxide (H_2O_2) as oxidant, as illustrated in the present work, is a right choice for polymerization to happen, which not only eliminates the toxicity issues but generates nanostructured polypyrrole, with particle size much smaller than the ones synthesized using conventional routes [26]. The synthesis method of polypyrrole, adopted in the present work can hence be considered as an ecofriendly method most appropriate for biomedical applications.

Curcumin is a well-known hydrophobic, yellow-orange colored natural polyphenol derived from the rhizome of the herb *Curcuma longa* commonly known as turmeric, which is a dietary spice as well as an herbal supplement [29]. This Indian spice has a long history of use in Ayurvedic medicine because of its anti-inflammatory, antimicrobial, and anti-carcinogenic activity and a host of healing properties for the treatment of most diseases [30–35]. Several studies indicate that curcumin is a potent anticancer agent because of its capability to suppress the proliferation of many types of tumor cells [36, 37]. Moreover, it is inexpensive and has been found to be safe in human clinical trials and reported to be nontoxic in animals and humans even at high doses. However, the poor aqueous solubility and high rate of metabolism significantly limit its bioavailability and clinical efficacy [38]. Reduced bioavailability of curcumin can be related to its poor absorption and high rate of metabolism caused by the enzymes present in the intestinal tract and rapid systemic elimination [39]. These factors significantly limit its bioavailability and clinical efficacy in pharmaceutical formulations. An improvement in the stability and solubility of curcumin is essential to overcome these difficulties. Developing novel, nanoparticle-based DDSs which can encapsulate hydrophobic drugs like curcumin could be

a solution to overcome these limitations [10, 11]. Significant increase in the oral bioavailability of curcumin has been reported by different research groups when curcumin is encapsulated within nanoparticles. This kind of DDSs have the advantage that they carry far less amount of drugs, but offer systemic localized availability of drugs which results in improved therapeutic effects and protective measures [40, 41].

Present study is focused on assessing the prospects of the nanocomposite of polypyrrole (PPy) and functionalized multi-walled carbon nanotubes (f-MWCNTs) as a smart drug carrier system for drug delivery applications, using curcumin as the model drug. Here we report an ecofriendly route for the synthesis of PPy/f-MWCNTs nanocomposite using initially functionalized MWCNTs. Functionalization of MWCNTs has been carried out using a green approach in which lemon extract is used as the oxidizing medium instead of strong acids. Oxidation of MWCNTs in lemon juice results in the fragmentation of MWCNTs into nanoscale dimensions with their caps removed which facilitates drug loading through sonication. Monomer pyrrole is polymerized in the presence of f-MWCNTs, using H_2O_2 as the oxidant. The nanocomposite thus formed consists of f-MWCNTs wrapped by the spongy structured PPy, which prevents the uncontrolled leakage of drug through the open ends of the tubes, ensuring controlled release of the drug. The synthesized nanocomposite shows enhanced encapsulation efficiency of about 89% and sustained and pH dependent release of the drug over a period of one week. The nanocomposite is found to be non-toxic and compatible toward normal cells as per the results obtained from cytotoxicity studies. The cellular uptake of the nanocomposite further strengthens the suitability of f-MWCNTs/PPy nanocomposite as an efficient drug delivery system. The green chemistry route followed in the synthesis of the nanocomposite of the present work has proved to be an efficient and nontoxic approach for developing novel types of drug delivery systems for the controlled release of drugs and is being reported for the first time through this article.

Experimental

Materials

Monomer pyrrole (99%) was purchased from Sigma-Aldrich and purified through distillation under reduced pressure and stored in refrigerator before use. Multi-walled carbon nanotubes (MWCNTs) with 95% purity and average diameter around 35–45 nm and length of a few micrometers were obtained from Graphene Super market, USA. All other reagents including hydrogen peroxide (Sigma Aldrich), sodium dodecyl sulfate (Merck), sodium hydroxide (Merck) and hydrochloric acid (Merck) were used as received. Curcumin was purchased from Merck India Limited. Dulbecco's modified eagle medium (DMEM) and sulforhodamine B (SRB) were purchased from Sigma-Aldrich. Human breast cancer cell line (MD-MBA) for cellular up take studies was purchased from NCCS, Pune. All the chemicals used were of analytical grade.

Methods

Functionalization of MWCNTs and curcumin loading

Multi-walled carbon nanotubes (MWCNTs) were functionalized using lemon extract as follows. Fresh lemons were washed thoroughly in deionized water and the juice was extracted. The extract was first filtered in a sieve and the subsequent filtration was done using Watman filter paper to get clear juice. In a typical case, MWCNTs (25 mg) were refluxed in 20 ml of lemon extract for six hours at 80 °C. The resulting mixture was then allowed to cool and was washed several times in deionized water till neutral pH was achieved and then dried in a vacuum oven at 60 °C. Upon drying, black colored, functionalized MWCNTs (f-MWCNTs) were obtained in powder form.

Initially a stock solution of curcumin was prepared in ethanol at a concentration of 2 mg/ml. Then 10 mg of f-MWCNTs was dispersed in 10 ml of sterilized deionized water and sonicated for 20 min. Curcumin stock solution was added to the dispersion f-MWCNTs and the mixture was again sonicated for 20 min in order to get the curcumin solution pushed inside the nanotubes through their open ends.

Synthesis of f-MWCNTs/PPy nanocomposite and curcumin loaded nanocomposite

In a typical synthesis, 30 ml of 0.1 molar HCl solution was added to the dispersion of f-MWCNTs in de-ionized water and kept for stirring. The dopant, sodium dodecyl sulfate (300 mg) was dissolved in 10 ml of 0.1 molar HCl and the resulting solution was added to the f-MWCNTs solution under stirring conditions to which 0.84 ml of monomer pyrrole was added. After one hour, 3 ml of hydrogen peroxide (H₂O₂) was added. The solution was found to turn black with the addition of H₂O₂. Stirring was continued for 24 h to ensure complete polymerization of pyrrole monomer to yield f-MWCNTs/PPy nanocomposite. Resulting nanocomposite was separated from the suspension by high speed centrifugation and was washed in distilled water and air dried. Same synthesis procedure was repeated to obtain PPy/curcumin loaded f-MWCNTs nanocomposite in powder form. For comparison, PPy loaded with the drug, curcumin, was also synthesized following similar procedure.

Characterization

Surface morphology of drug loaded f-MWCNTs/PPy nanocomposite was studied with the help of field emission scanning electron microscopy (FESEM) using JEOL Model JSM—6390LV machine and transmission electron microscopy (TEM) using JEOL model JEM- 2100 machine having resolution of 0.24 nm and an acceleration voltage of 200 kV. Interaction of the drug with the nanocomposite was confirmed from Fourier transform infrared spectroscopic (FTIR) studies, conducted using AVTAR 370 DTGS FTIR spectrophotometer in the range 400–4000 cm⁻¹. X-ray diffraction patterns were obtained on Rigaku X-ray diffractometer with Cu K α (λ =1.5481Å) radiation

operating at 30 kV and 20 mA at a scan speed of 2° per minute in the range 10°–70°. Size distribution of f-MWCNTs/PPy nanocomposite samples with and without drug loading was analyzed by dynamic light scattering (DLS) technique using Nicomp TM380 ZLS machine and stability of the nanocomposite samples was assessed by zeta potential measurements, carried out using the same instrument. Cellular uptake of drug loaded nanocomposite was established on the basis of fluorescence images obtained using fluorescent microscope Nikon-Eclipse.

Entrapment efficiency and loading efficiency

Entrapment efficiency and loading efficiency of curcumin within f-MWCNTs/PPy nanocomposite were determined using the supernatant collected after centrifugation of the drug loaded nanocomposite. Amount of un-entrapped curcumin in the supernatant was quantified spectrophotometrically at an absorption maximum of 428 nm, which corresponds to the peak absorption of curcumin. Quantity of free curcumin present in the supernatant gives the total amount of un-entrapped curcumin. Encapsulation efficiency or entrapment efficiency (EE) can then be expressed as the percent of the entrapped curcumin, based on the ratio of the amount of curcumin present in the nanocomposite to the amount of curcumin added [40].

$$EE (\%) = (\text{Total drug added} - \text{Diffused drug}) / (\text{Total drug added}) \times 100$$

Loading efficiency (LE) of the drug-loaded composite was calculated with respect to the yield of the nanocomposite, obtained after centrifugation.

$$LE (\%) = (\text{Total amount of curcumin entrapped} / \text{Yield of drug loaded nanocomposite}) \times 100$$

In vitro drug release studies

In vitro drug release studies of drug loaded nanocomposite were carried out using direct dispersion method at neutral (7.4) and acidic (4.5) pH conditions over a period of one week. A known quantity of curcumin loaded nanocomposite was dispersed in 20 ml phosphate-buffered saline (PBS) and the dispersion was incubated in a water bath shaker at 37 °C under gentle shaking. At proper time intervals, the supernatants were collected and were replaced by equivalent volumes of fresh PBS solution. Curcumin in the nanocomposite was first extracted in ethanol and quantified spectrophotometrically at a wavelength of 428 nm. Drug release profile of curcumin loaded f-MWCNTs/PPy nanocomposite was studied at a pH of 7.4 and also at acidic pH of 4.5. Percentage release of curcumin was determined as [42].

Curcumin release (%)

$$= ((\text{Curcumin released at time } t) / (\text{total curcumin loaded in nanocomposite})) \times 100$$

In vitro cellular uptake studies using fluorescent imaging

In vitro cellular uptake studies of curcumin loaded f-MWCNTs/PPy nanocomposite were done by fluorescent imaging as follows. Human breast cancer cells (adenocarcinoma cell monolayer MDA-MB-231) were seeded in to 12 well plates at a density of 1×10^4 cells per well. Cells were cultured at 37 °C in 5% CO₂ in Dulbecco's Modified Eagle's Medium (DMEM) supplemented with 10% fetal bovine serum (FBS). In a typical study, 1 mg of drug loaded nanocomposite was dispersed in 2 ml of PBS and subjected to probe sonication for 5–10 s. Cells were then incubated with 50 μ l of the sonicated nanocomposite solution. Following two hours of exposure of cells to the nanocomposite, the sample containing media was completely removed and the unbound nanocomposite sample was rinsed off with a PBS wash. Subsequently, the cells were fixed in 4% paraformaldehyde in PBS and imaged with an advanced inverted fluorescent microscope (Nikon-Eclipse TE 2000-S). Images were captured for excitations at 470 nm and 514 nm using a multiline solid state laser system (470, 514 nm) and appropriate filter band (blue, green) combinations.

In vitro cytotoxicity studies using SRB (sulphrodamine B) assay

Sulphrodamine B (SRB) assay was used to study the cytotoxicity effects of f-MWCNTs/PPy nanocomposite. Human lung cancer cell line NCI-H460 maintained in RPMI-1640 medium supplemented with 10% (v/v) fetal bovine serum (FBS) at 37 °C with 5% carbon dioxide (CO₂) was used for the assay. Aliquots of 190 μ L cell suspension with a density of 1.9×10^4 cells were pipetted into 96 well micro titer plates. Nanocomposite was dissolved in sterile de-ionized water with initial stock concentration of 4 mg/mL. Subsequently two fold serial dilutions of the stock were prepared with concentration ranging from 4 mg/mL to 250 μ g/mL in sterile de-ionized water. Then, 10 μ L of each of these samples was added to each well so as to get a final concentration ranging from 200 to 12.5 μ g /mL. Control group was included having cells with 10 μ L de-ionized water alone instead of extract. The plates were then incubated at 37 °C in a CO₂ (5%) incubator for 48 h, and then fixed with 100 μ L ice cold, 30% trichloroacetic acid (TCA) and further incubated at 4 °C for another 1 h. Plates were then gently washed and air dried at room temperature. To each well, 100 μ L, 0.057% (wt/vol) SRB prepared in de-ionized water with 1% acetic acid was added and left at room temperature for 30 min. Unbound stain was washed off by using 1% acetic acid and each well was air dried further. To dissolve the cell bound dye, 200 μ L of 10 mM Tri base solution (pH 10.5) was added to each well and the plate was shaken on a gyratory shaker for 10 min and optical density (OD) was read at 510 nm in a microplate reader (Tecan) [43].

Percentage of cell-growth inhibition (GI) was calculated as per the following equation.

$$\text{Percentage of growth inhibition} = 100 - \text{Percentage of control cell growth}$$

Percentage of control cell growth

$$= ((\text{Mean OD of sample} - \text{Mean OD for day 0}) / ((\text{Mean OD of negative control} - \text{Mean OD for day 0})) \times 100$$

Curcumin induced cell death analysis

To examine the therapeutic activity of curcumin encapsulated nanocomposite under in vitro conditions, a monolayer of human breast cancer derived cells was exposed to drug containing f-MWCNTs/PPy nanocomposite. Here, propidium iodide (PI)-based nuclear stain was used to understand the extent and mode of cell death through fluorescence microscopic image analysis. Briefly, MDA-MB-231 cells were seeded at a density of 2×10^5 in three separate chamber glass slides. The cells were grown to 70% confluence in an incubator at 37 °C in a humidified atmosphere of 5% CO₂. Subsequently, 1 mg of nanocomposite sample was weighed and dispersed in 2 ml of PBS and subjected to probe sonication for 5 s. An aliquot of 100 µl of this sonicated sample was added to the monolayer of MDA-MB cells. Curcumin encapsulated nanocomposite sample was exposed to cells in the presence of serum containing medium for time periods of 24 h, 48 h and 92 h. At the end of each stipulated time point, the medium was removed from one of the chamber slides and the cells were washed with PBS. Subsequently, 5 µl of 0.1 µg/ml concentration of PI solution was used to stain the cells. The cells were incubated for 10 min in the incubator before obtaining fluorescent images [44].

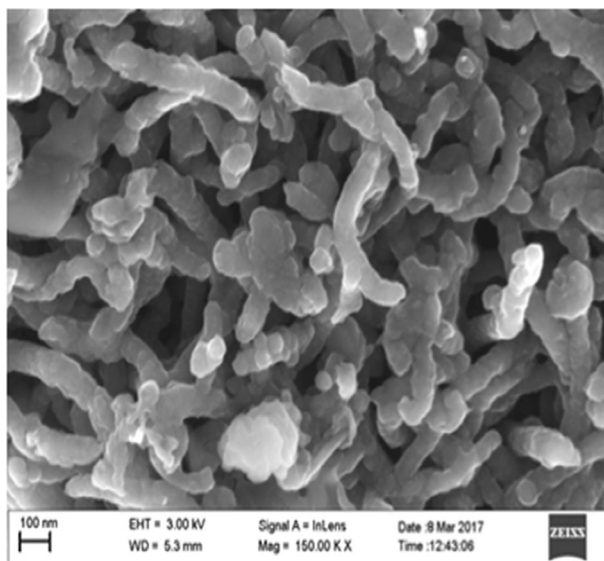


Fig. 1 FESEM image of drug loaded f-MWCNTs/PPy nanocomposite

Results and discussions

FESEM and TEM analysis

FESEM image of drug loaded f-MWCNTs/PPy nanocomposite shows a tubular morphology in which f-MWCNTs fragments are found to be completely wrapped by the porous structured PPy as evident from Fig. 1. In the present case, MWCNTs are functionalized using lemon extract instead of doing conventional acid functionalization. Refluxing of MWCNTs in lemon juice at elevated temperature facilitates effective oxidation of MWCNTs due to the presence of high content of citric acid in lemon [45, 46]. Oxidation process initially removes the nanotube caps followed by cutting of the nanotubes to nanoscale fragments. Average diameter of MWCNTs used in the present study is around 40 nm (as per the label on the purchased bottle) and the size of the synthesized f-MWCNTs/PPy nanocomposite is found to be around 65 nm. This observation clearly indicates that f-MWCNTs fragments are covered by nanometer scale layer of polypyrrole. Main challenge associated with CNTs assisted drug delivery systems is the chance of leaking out of the drug through the open ends of functionalized CNTs, which results in uncontrolled release of drug. In many practical applications, controlled release of drug is required and preferred. Under such situations, morphology of f-MWCNTs/PPy nanocomposite of the present work is the most appropriate one, because the porous covering of PPy over f-MWCNTs, prevents uncontrolled leaking of the drug and facilitates its controlled release by sealing the open ends of the nanotubes.

TEM image of drug loaded f-MWCNTs/PPy nanocomposite is shown in Fig. 2. Nanotube fragments are filled with the drug containing solution, which is

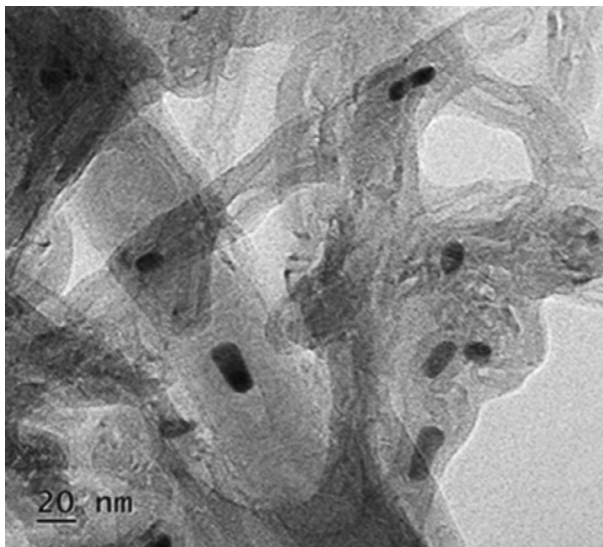


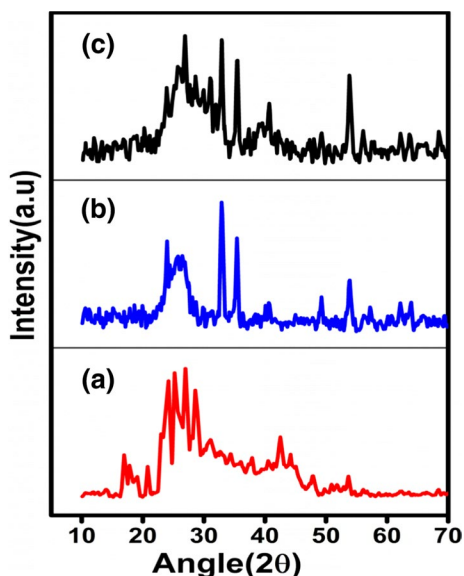
Fig. 2 TEM image of drug encapsulated f-MWCNTs/PPy nanocomposite

found to be coalesced to form bigger droplets inside the void spaces of the nanotubes, as revealed from the figure. Removal of the caps of nanotubes during functionalization facilitates their application as molecular containers, which results in enhanced encapsulation efficiency. In addition, presence of oxygen containing functional groups on the open ends and surfaces of nanotubes makes the surfaces of MWCNTs more hydrophilic and facilitates easy loading of drug solution to the interiors of the tubes through sonication. Many of the earlier reports are based on integrating the drug molecules to be delivered to the functional groups on the surfaces of f-MWCNTs, through covalent or non-covalent bonding, leaving the inner voids of the MWCNTs unutilized. When the caps of the MWCNTs are removed as seen in the present work, the inner voids of the tubes are also made available, which helps to load more amount of drugs. Presence of outer porous covering of polypyrrole further facilitates slow and steady release of the loaded drug.

XRD analysis

XRD patterns of bare curcumin, f-MWCNTs/PPy nanocomposite and curcumin loaded PPy/ f-MWCNTs nanocomposite are shown in Fig. 3. As can be seen from the figure, pure curcumin exhibits sharp, characteristic peaks in the range of 15° – 30° , inferred to traits of a high crystalline structure [31, 35]. Plot of f-MWCNTs/PPy nanocomposite consists of amorphous as well as crystalline regions, with the crystalline peaks corresponding to the ordered regions and the broad ones to the amorphous regions of the nanocomposite. Observed sharp diffraction peaks are signatures of structural ordering in the nanocomposite when

Fig. 3 XRD patterns of **a** curcumin **b** f-MWCNTs/PPy nanocomposite and **c** curcumin loaded f-MWCNTs/PPy nanocomposite



f-MWCNTs are attached to the polymer back bone. The peak at 26.4° is relatively broad and intense, because in this region the characteristic peak of polypyrrole and the graphitic peak of MWCNTs merge together [47–49]. Diffraction pattern of curcumin loaded f-MWCNTs/PPy nanocomposite is characterized by the absence of some of the prominent curcumin peaks which is a clear evidence of the encapsulation of curcumin within the f-MWCNTs/PPy nanocomposite.

FTIR spectroscopic studies

Fourier transform infrared (FTIR) spectroscopy is one of the important characterization techniques to study the interactions and perturbations that occur in the drug loaded polymer nanocomposite. The FTIR spectra of free curcumin, f-MWCNTs/PPy nanocomposite and curcumin loaded f-MWCNTs/PPy nanocomposite are shown in Fig. 4. In the spectrum of curcumin, the band at 3505 cm^{-1} is attributed to the phenolic O–H stretching vibration. The band at 1632 cm^{-1} corresponds to stretching vibrations of the benzene ring of curcumin. The one at 1507 cm^{-1} can be attributed to C=C vibrations and that at 1281 cm^{-1} to aromatic C–O stretching vibrations. The band at 1032 cm^{-1} corresponds to the stretching modes of keto group of curcumin and the one at 809 cm^{-1} represents C–O–C stretching vibrations of curcumin [50]. In the spectrum of f-MWCNTs/PPy nanocomposite, the less intense peak at 3123 cm^{-1} indicates the presence of –OH groups attached to functionalize MWCNTs. The peak at 1702 cm^{-1} can be assigned to C=O stretching mode of –COOH groups which indicates the carboxyl group functionalization of MWCNTs. The one at 1562 cm^{-1} corresponds to C=C stretching vibrations of pyrrole ring and that at 1309 cm^{-1} results from C–N stretching vibrations of PPy due to the interaction between PPy and MWCNTs.

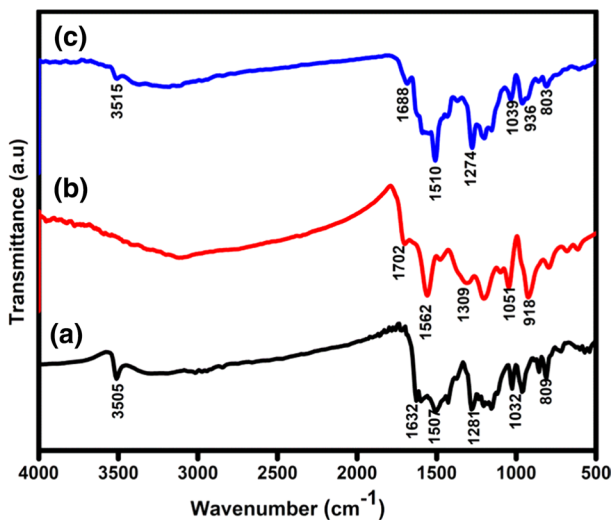


Fig. 4 FTIR spectra of **a** curcumin **b** f-MWCNTs/PPy nanocomposite and **c** curcumin loaded f-MWCNTs/PPy nanocomposite

Fig. 5 Particle size distribution of f-MWCNTs/PPy nanocomposite

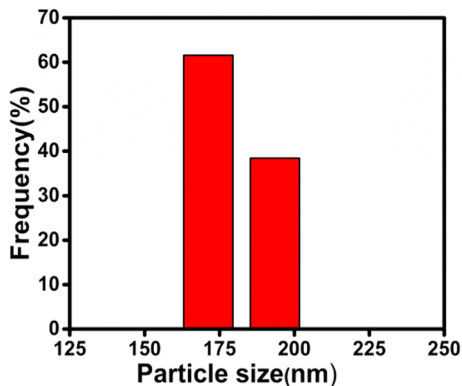
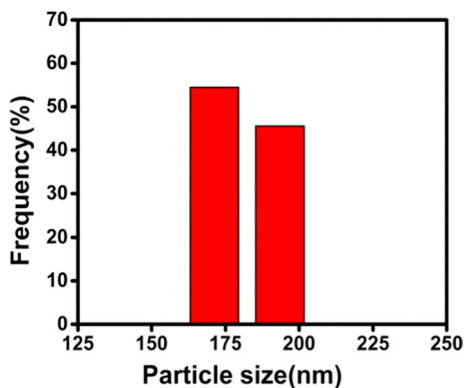


Fig. 6 Particle size distribution of curcumin loaded f-MWCNTs/PPy nanocomposite



The bands at 1051 cm^{-1} and 918 cm^{-1} are due to the out-of-plane and in-plane vibrations of $=\text{C}-\text{H}$ in PPy [51]. The spectrum of curcumin loaded nanocomposite shows bands corresponding to polypyrrole, f-MWCNTs and curcumin, but there are shifts in peak positions and changes in peak intensities, which indicate that some kind of interaction occurs between the nanocomposite and the drug.

Particle size analysis using dynamic light scattering (DLS) and stability studies by zeta potential measurements

Particle size distribution of f-MWCNTs/PPy nanocomposite and curcumin loaded f-MWCNTs/PPy nanocomposite in aqueous solutions was determined using DLS measurements and the results are shown in Fig. 5 and Fig. 6, respectively. Particle size of f-MWCNTs/PPy nanocomposite lies in the range 170 to 190 nm with an average size of 180 nm and that of curcumin loaded f-MWCNTs/PPy nanocomposite lies within a size range of 172 to 194 nm with an average size of 183 nm. There is no appreciable difference in the particle size of the drug loaded nanocomposite, compared to the one without drug loading as revealed from the DLS data. Generally, in nanoparticle-based drug delivery systems, the nanoparticles

are of spherical morphology and the drug is encapsulated within the nanoparticles as well as absorbed by their surfaces, so that significant difference in the size of the drug loaded and bare nanoparticles is observed [24]. But the nanocomposite-based drug delivery system of the present study involving f-MWCNTs is of tubular morphology in which the inner voids of f-MWCNTs are utilized for storing the drug and hence no significant change in the size of the drug loaded nanocomposite and bare nanocomposite has been observed [21]. The average particle size of 183 nm observed in the present work for the drug loaded nanocomposite will be ideal for cell internalization, since majority of tumors exhibit a vascular pore cut-offs between 380 and 780 nm [35].

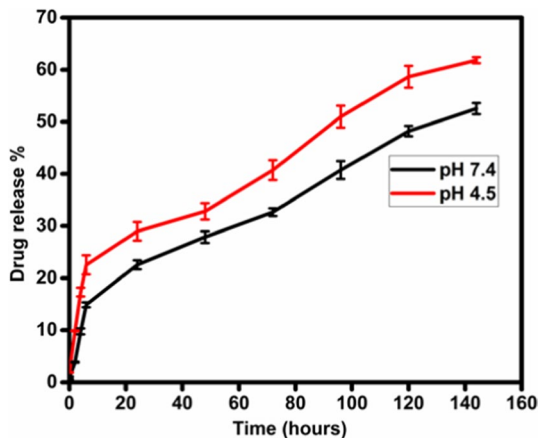
Surface charge is one of the factors determining the physical stability of nanoparticles in colloidal systems and can be evaluated using zeta potential measurements. If the particles bear a higher value of the same charge, making the electrostatic repulsion between the particles greater, the chances of aggregation can be reduced which brings about higher stability to the nanoparticles [52]. The zeta potential values obtained for curcumin loaded f-MWCNTs/PPy nanocomposite and bare nanocomposite are 18.4 mV and -6.3 mV, respectively. The high positive zeta potential value shown by curcumin loaded nanocomposite, compared to bare nanocomposite indicates good colloidal stability of the drug loaded nanocomposite system because this value lies well within the stable range. In addition to having ideal size, presence of a highly positive surface charge on the drug loaded nanocomposite facilitates effective cellular uptake since the nanocomposite, through electrostatic interactions can bind with the negatively charged cell membranes and subsequent internalization becomes easier [53].

Entrapment efficiency and in vitro drug release studies

Main objective of the present study is to develop a better nanocarrier system with high drug loading capacity, capable of offering controlled and sustained release of drug for a sufficiently long period of time. These two factors have been recognized as most important for an efficient drug delivery system [2, 8]. Drug loaded, f-MWCNTs/PPy nanocomposite, developed in the present work fulfills these requirements and shows not only enhanced entrapment efficiency but slow and controlled release of the drug as well. Encapsulation and loading efficiencies of curcumin loaded f-MWCNTs/PPy nanocomposite of the present study have been estimated as 89% and 5.11% respectively whereas the encapsulation efficiency of curcumin loaded PPy, without f-MWCNTs is 67%. Enhanced encapsulation efficiency of curcumin loaded, f-MWCNTs/PPy nanocomposite can be attributed to the effective utilization of inner void spaces of the f-MWCNTs, for storing the drug solution.

Release profiles of curcumin from curcumin loaded f-MWCNTs/PPy nanocomposite at pH values of 7.4 and 4.5 are shown in Fig. 7. Initial release of the drug is very slow, but later it gets increased to about 23% at pH 7.4 and 29% at pH 4.5 in the first 24 h and this observed burst release might be due to the dissociation of the drug adsorbed on the outer surfaces of the spongy textured outer PPy layer, which does

Fig. 7 Drug release profiles of curcumin loaded f-MWCNTs/PPy nanocomposite at neutral and acidic pH conditions



not get in to the inner voids of the nanotubes. The initial burst release is followed by a slow and steady release of the drug for the next six days. It can be seen that at physiological pH 7.4, only 53% of the total encapsulated drug is released within a period of one week, so that the remaining drug can be expected to be released in the next few days. This observed slow release of drug from f-MWCNTs/PPy nanocomposite can be attributed to the longer time taken by the drug molecules trapped inside the hollow cylinders of f-MWCNTs to come out, which are further covered by the polymer matrix. Drug loaded nanocomposite shows a slower release at physiological pH, compared to the acidic pH environment, which is expected [35, 40]. In the acidic environment (pH 4.5), higher drug released of about 62% is observed compared to that under neutral pH, as depicted in Fig. 7. This is due to the swelling of the polymer matrix in the acidic environment produced by the protonation of the polymer back bone. As polypyrrole is a conducting polymer, at acidic pH, the outer polypyrrole covering around the nanotubes gets protonated which will increase the net positive charge on the polymer back bone. The repulsive force produced by the neighboring positive charges results in a stress on the nanotubes, pushing out more amount of drug at a faster rate [26]. The obtained drug release pattern demonstrates an increase in the release of the drug with a decrease in pH. This pH sensitive release of curcumin is advantageous in cancer therapy because the pH environment of the biological fluid surrounding the tumor site is usually acidic, and the pH value is much lower than that of normal tissues [35]. This will facilitate a faster release of drug from the nanoparticle-based drug delivery system to the tumor sites and will also reduce the undesired drug release during the transportation of the drug through regions where physiological pH exists.

In vitro cell uptake studies using fluorescent imaging

In vitro cellular uptake studies of curcumin loaded f-MWCNTs/PPy nanocomposite were carried out, using fluorescence microscopy technique by envisaging the

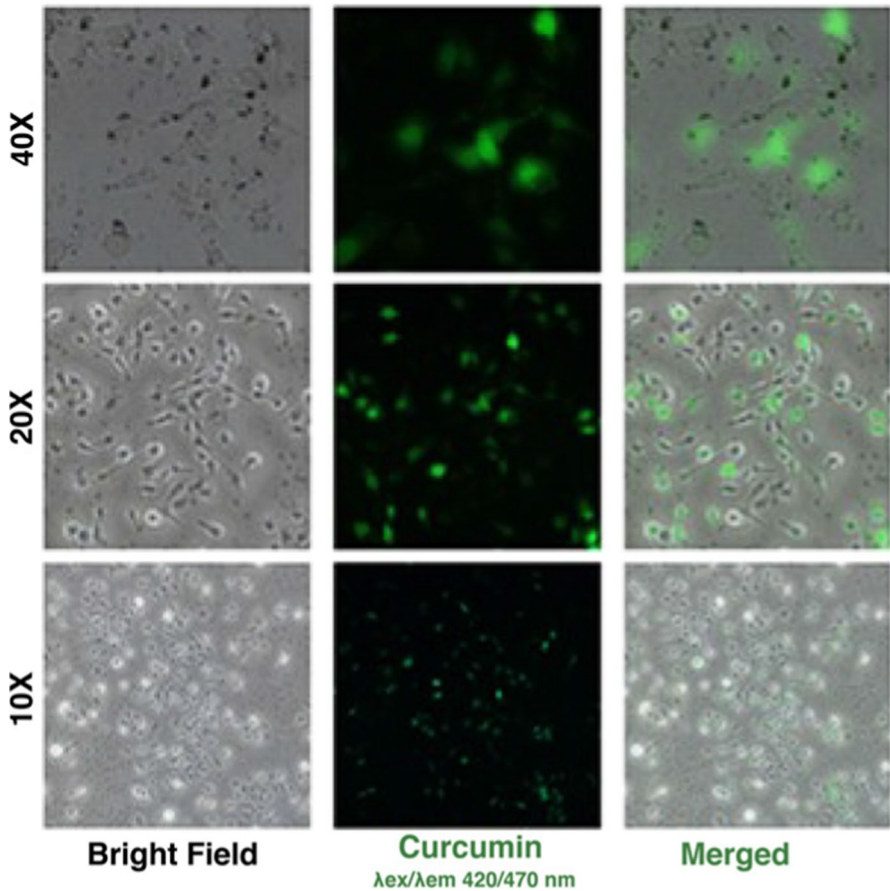


Fig. 8 Fluorescence microscopic images showing the cellular uptake of curcumin loaded f-MWCNTs/PPy nanocomposite by MDA-MB-231 cells

intrinsic fluorescence of curcumin. Microscopic images of human breast cancer cell lines (adenocarcinoma cell monolayer MDA-MB-231) after 2 h of incubation with the drug loaded f-MWCNTs/PPy nanocomposite are shown in Fig. 8. Images captured following excitation at 470 nm and 514 nm, using appropriate filter band (blue, green) combinations are also shown. Green fluorescence in the microscopic images confirms the internalization of curcumin from the nanocomposite matrix to the cells.

Curcumin induced cell death analysis

Chemotherapeutic potency of curcumin loaded f-MWCNTs/PPy nanocomposite at the preliminary in vitro level was studied in human adenocarcinoma derived cell lines. Propidium iodide (PI), the classic membrane, nucleic acid dye served as the live/dead cell discriminator. Gradual increase in the permeability of this dye through

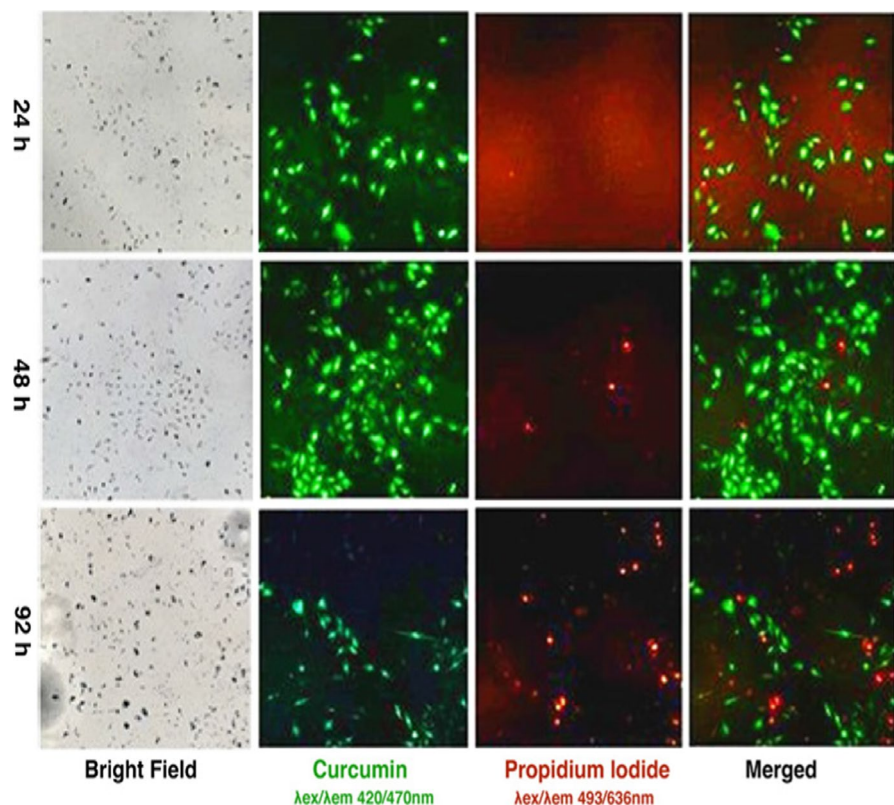


Fig. 9 Fluorescent images of MDA-MB-231 cells taken at 24, 48 and 92 h of incubation

the compromised integrity of plasma membrane, visualized as red fluorescence is a semaphore in cell death, especially at the end stages of apoptosis. The pleiotropic polyphenol, curcumin is known to induce apoptotic cell death in breast cancer cell population in a dose dependent manner. Correspondingly, fluorescent microscopic images shown in Fig. 9 illustrates the anticancer potential of curcumin that gets diffused into the cancerous cells after 24 h, 48 h and 92 h of nanocomposite incubation. The figure clearly depicts a time dependent increase in the number of red fluorescent spots in the microscopic images as indicative of the dead cell population. This basically reflects the release trend of curcumin from the nanocomposite system where its cumulative accumulation after 92 h produces significant therapeutic effect.

Naturally, after 24 h of incubation, no significant toxicity has been observed but the green fluorescence seen in cells indicates the initiation of curcumin release and cellular uptake. Hitherto, after 48 h of incubation a gradual increase in the number of dead cells is observed which culminates at 92 h of time period. This result reveals that drug release from f-MWCNTs/PPy nanocomposite is very slow and corroborates with the drug release profile already. This slow, continuous release pattern of the drug from the nanocomposite system to the cells highlights the therapeutic potential of curcumin loaded f-MWCNTs/PPy nanocomposite against cancerous cells.

In vitro cytotoxicity evaluation by SRB assay

Generally in drug release studies, ensuring nontoxicity of the drug carrier in the physiological medium is mandatory and is extremely important. Cytotoxicity studies of f-MWCNTs/PPy nanocomposite were carried out to establish the low toxicity of the nanocomposite toward live cells. Cytotoxicity evaluation of f-MWCNTs/PPy nanocomposite at different concentrations was conducted using SRB assay and the results are shown in Fig. 10.

It is evident from the figure that the synthesized nanocomposite shows high cell viability even for high concentrations of the nanocomposite. Percentage cell viability for lowest concentration of the composite is near to 100%, showing zero toxicity. At the highest concentration of 200 $\mu\text{g}/\text{mL}$, the nanocomposite shows very little toxicity less than 4% toward the cells, establishing the excellent biocompatibility of the nanocomposite. High percentage of cell viability shown by the nanocomposite of the present work may be attributed to the green strategy adopted for the synthesis of the nanocomposite.

Conclusions

A novel drug delivery system involving the nanocomposite of polypyrrole (PPy) and functionalized MWCNTs, loaded with the drug, curcumin has been developed by chemical in situ polymerization of pyrrole, in the presence of curcumin loaded, functionalized MWCNTs (f-MWCNTs), following ecofriendly synthesis routes. Functionalization of MWCNTs has been carried out using lemon extract and the nanocomposite of polypyrrole and f-MWCNTs is used as drug carrier, exploiting the inner void spaces of f-MWCNTs as storage places for the drug, which can provide enhanced encapsulation efficiency. Porous covering of PPy over f-MWCNTs not only helps to eliminate unwanted leakage of drug from the f-MWCNTs but facilitates the controlled release of drug for a prolonged period as well, increasing the therapeutic efficacy of the

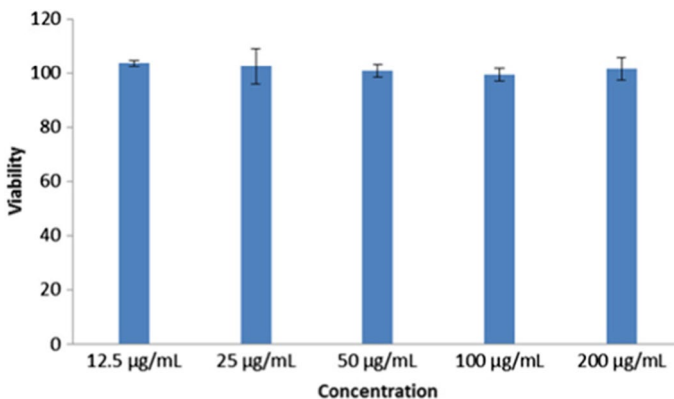


Fig. 10 Cytotoxicity evaluation of f-MWCNTs/PPy nanocomposite at different concentrations

nanocomposite. X-ray diffraction and FTIR spectroscopic studies confirm the presence of curcumin within the drug loaded nanocomposite. In addition, the synthesized nanocomposite system shows high positive zeta potential indicating good colloidal stability. In vitro drug release studies indicate slow, controlled and sustained release of drug from the nanocomposite matrix. Cellular internalization of drug loaded f-MWCNTs/PPy nanocomposite has been confirmed from the green fluorescence observed in the microscopic images of human breast cancer cells. Excellent cell viability shown by the nanocomposite establishes the non-toxic nature of the nanocomposite as revealed from the cytotoxicity studies. Curcumin induced cell death analysis of cancerous cells shows a time dependent increase in the number of dead cells, establishing the chemotherapeutic potency of curcumin loaded f-MWCNTs/PPy nanocomposite. These results suggest that f-MWCNTs/PPy nanocomposite of the present work, synthesized through green approaches can be used as an ideal and effective carrier to deliver hydrophobic drugs like curcumin, and thus offers great promise in drug delivery applications.

Acknowledgements Authors, P. Saheeda (Grant Number: KLCA028TF19) and K. Sabira, gratefully acknowledge University Grants Commission, Government of India for providing teacher fellowship under Faculty Improvement Program.

Declarations

Conflict of interest The authors declare that they have no known competing financial interests or personal relationships that could have appeared to influence the work reported in this paper.

References

1. Lombardo D, Kiselev MA, Caccamo MT (2019) Smart nanoparticles for drug delivery application: development of versatile nanocarrier platforms in biotechnology and nanomedicine. *J Nanomater.* <https://doi.org/10.1155/2019/3702518>
2. Patra JK, Das G, Fraceto LF, Campos EVR, Torres MPR et al (2018) Nano based drug delivery systems: recent developments and future prospects. *J Nanobiotechnol* 16:71. <https://doi.org/10.1186/s12951-018-0392-8>
3. Wilczewska AZ, Niemirowicz K, Markiewicz KH, Car H (2012) Nanoparticles as drug delivery systems-review. *Pharmacol Rep* 64:1020–1037
4. Zhang L, Gu FX, Chan JM, Wang AZ, Langer RS, Farokhzad OC (2008) Nanoparticles in medicine: therapeutic applications and developments. *Clin Pharmacol Ther.* <https://doi.org/10.1038/sj.clpt.6100400>
5. Hughes GA (2005) Nanostructure-mediated drug delivery. *Nanomed Nanotechnol Biol Med.* <https://doi.org/10.1016/j.nano.2004.11.009>
6. Nikalje AP (2015) Nanotechnology and its applications in medicine. *Med Chem* 5:2. <https://doi.org/10.4172/2161-0444.1000247>
7. Singh R, Lillard JW Jr (2009) Nanoparticle-based targeted drug delivery. *Exp Mol Pathol* 86(3):215–223. <https://doi.org/10.1016/j.yexmp.2008.12.004>
8. Sutradhar KB, Amin MdL (2014) Nanotechnology in cancer drug delivery and selective targeting. *ISRN Nanotechnol.* <https://doi.org/10.1155/2014/939378>
9. Yu X, Trase I, Ren M, Duval K, Guo X, Chen Z (2016) Design of nanoparticle-based carriers for targeted drug delivery. *J Nanomater.* <https://doi.org/10.1155/2016/1087250>
10. Mitchell MJ, Billingsley MM, Haley RM, Wechsler ME, Peppas NA, Langer R (2020) Engineering precision nanoparticles for drug delivery. *Nat Rev Drug Discov.* <https://doi.org/10.1038/s41573-020-0090-8>

11. Mohanty C, Sahoo SK (2010) The in vitro stability and in vivo pharmacokinetics of curcumin prepared as an aqueous nanoparticulate formulation. *Biomaterials* 31:6597–6611. <https://doi.org/10.1016/j.biomaterials.2010.04.062>
12. Mareeswaran MP, Babu E, Sathish V, Kim B, Woo SI et al (2014) p-Sulfonatocalix [4] arene as a carrier for curcumin. *J Chem* 38:1336. <https://doi.org/10.1039/c3nj00935a>
13. Balasubramanian K, Burghard M (2005) Chemically functionalized carbon nanotubes. *Small*. <https://doi.org/10.1002/smll.200400118>
14. Harris PJF (2004) Carbon nanotube composites. *Int Mater Rev* 49:31–43. <https://doi.org/10.1179/095066004225010505>
15. Heister E, Brunner EW, Dieckmann GR, Jurewicz I, Dalton AB (2013) Are carbon nanotubes a natural solution? Applications in biology and medicine. *ACS Appl Mater Interfaces* 5:1870–1891. <https://doi.org/10.1021/am302902d>
16. Bianco A, Kostarelos K, Partidos CD, Prato M (2005) Biomedical applications of functionalised carbon nanotubes. *Chem Commun*. <https://doi.org/10.1039/b410943k>
17. Yang W, Thordarson P, Gooding JJ, Ringer SP, Braet F (2007) Carbon nanotubes for biological and biomedical applications. *Nanotechnology* 18:412001. <https://doi.org/10.1088/0957-4484/18/41/412001>
18. Kumar R, Dhanawat M, Kumar S, Singh BN, Pandit JK, Sinha VR (2014) Carbon nanotubes: a potential concept for drug delivery applications. *Recent Pat Drug Deliv Formul*. <https://doi.org/10.2174/1872211308666140124095745>
19. Liu P (2013) Modification strategies for carbon nanotubes as a drug delivery system. *Ind Eng Chem Res* 52:13517–13527. <https://doi.org/10.1021/ie402360f>
20. ShengWong B, Yoong SL, Jagusiak A, Panczyk T, Ho HK, Ang WH, Pastorin G (2013) Carbon nanotubes for delivery of small molecule drugs. *Adv Drug Deliv Rev* 65:1964–2015
21. Luo X, Matraga C, Tan S, Alba N, Cui XT (2011) Biomaterials Carbon nanotube nanoreservoir for controlled release of anti-inflammatory dexamethason. *Biomaterials* 32:6316–6323. <https://doi.org/10.1016/j.biomaterials.2011.05.020>
22. Wang LX, Li XG, Yang YL (2001) Preparation, properties and applications of polypyrroles. *React Funct Polym* 47:125–139
23. Fonner JM, Forciniti L, Nguyen H, Byrne J, Kou YF, Nawaz JS, Schmidt CE (2008) Biocompatibility Implications of polypyrrole synthesis techniques. *Biomed Mater* 3(3):034124. <https://doi.org/10.1088/1748-6041/3/3/034124>
24. Wang J, Lin F, Chen J, Wang M, Ge X (2015) The preparation, drug loading and in vitro NIR photo-thermal-controlled release behavior of raspberry-like hollow polypyrrole microspheres. *J Mater Chem B* 3:9186–9193. <https://doi.org/10.1039/C5TB01314C>
25. Gao W, Li J, Cirillo J, Borgens R, Cho Y (2014) Action at a distance: functional drug delivery using electromagnetic-field-responsive polypyrrole nanowires. *Langmuir* 30:7778–7788. <https://doi.org/10.1021/la500033b>
26. Samanta D, Meiser JL, Zare RN (2015) Polypyrrole nanoparticles for tunable, pH-sensitive and sustained drug release. *Nanoscale*. <https://doi.org/10.1039/c5nr02196k>
27. Wang Y, Xiao Y, Tang R (2014) Spindle-like polypyrrole hollow nanocapsules as multifunctional platforms for highly effective chemo—photothermal combination therapy of cancer cells in vivo. *Chem Eur J* 20:11826–11834. <https://doi.org/10.1002/chem.201403480>
28. Rahman NA, Ishak T, Kudin T, Ali AMM (2012) Yahya MZA (2012) Synthesis and characteristics of conducting polymer- based polypyrrole in different solvents. *J Mater Sci Eng A* 2(2):190–195
29. Priyadarsin KI (2014) The chemistry of curcumin: from extraction to therapeutic agent. *Molecules* 19:20091–20112. <https://doi.org/10.3390/molecules191220091>
30. Aggarwal B, Harikumar KB (2009) Potential therapeutic effects of curcumin, the anti-inflammatory agent, against neurodegenerative, cardiovascular, pulmonary, metabolic, autoimmune and neoplastic diseases. *Int J Biochem Cell Biol* 41(1):40–59. <https://doi.org/10.1016/j.biocel.2008.06.010>
31. Yen FL, Wu TH, Wei C, Tzeng LLT, Lin CC (2010) Curcumin nanoparticles improve the physico-chemical properties of curcumin and effectively enhance its antioxidant and antitheatoma activities. *J Agric Food Chem* 58:7376–7382. <https://doi.org/10.1021/jf100135h>
32. Malik P, Mukherjee TK (2014) Structure-function elucidation of antioxidative and prooxidative activities of the polyphenolic compound curcumin. *Chin J Biol*. <https://doi.org/10.1155/2014/396708>
33. Nguyen VC, Nguyen VB, Hsieh MF (2013) Curcumin-loaded chitosan/gelatin composite sponge for wound healing application. *Int J Polym Sci*. <https://doi.org/10.1155/2013/106570>

34. Yang X, Li Z, Wang N, Li L, Song L, He T et al (2015) Curcumin-encapsulated polymeric micelles suppress the development of colon cancer in vitro and in vivo. *Sci Rep* 5:10322. <https://doi.org/10.1038/srep10322>
35. Anitha A, Deepagan VG, Rani VVD, Menon D, Nair SV, Jayakumar R (2011) Preparation, characterization, in vitro drug release and biological studies of curcumin loaded dextran sulphate—chitosan nanoparticles. *Carbohydr Polym* 84:1158–1164. <https://doi.org/10.1016/j.carbpol.2011.01.005>
36. Yallapu MM, Jaggi M, Chauhan SC (2012) Curcumin nanoformulations: a future nanomedicine for cancer. *Drug Discov Today* 17(1–2):71–80. <https://doi.org/10.1016/j.drudis.2011.09.009>
37. Bansal SS, Goel M, Aqil F, Vadhanam MV, Gupta RC (2011) Advanced drug-delivery systems of curcumin for cancer chemoprevention. *Cancer Prev Res (Phila)* 4(8):1158–1171. <https://doi.org/10.1158/1940-6207.CAPR-10-0006>
38. Dutt AK, Ikiki E (2013) Novel drug delivery systems to improve bioavailability of curcumin. *J Bioequiv Availab* 6:1. <https://doi.org/10.4172/jbb.1000172>
39. Pinheiro AC, Lad M, Silva HD, Coimbr M, Boland M, Vicente A (2013) Unravelling the behavior of curcumin nanoemulsions during in vitro digestion: effect of the surface charge. *Soft Matter* 9:3147–3154. <https://doi.org/10.1039/c3sm27527b>
40. Anitha A, Maya S, Deepa N, Chennazhi KP, Nair SV, Tamura H et al (2011) Efficient water soluble O-carboxymethyl chitosan nanocarrier for the delivery of curcumin to cancer cells. *Carbohydr Polym* 83:452–461. <https://doi.org/10.1016/j.carbpol.2010.08.008>
41. Shaikh J, Ankola DD, Beniwal V, Singh D, Kumar MNVR (2009) Nanoparticle encapsulation improves oral bioavailability of curcumin by at least 9-fold when compared to curcumin administered with piperine as absorption enhancer. *Eur J Pharm Sci* 37:223–230. <https://doi.org/10.1016/j.ejps.2009.02.019>
42. Das RK, Kasoju N, Bora U (2010) Encapsulation of curcumin in alginate-chitosan-pluronic composite nanoparticles for delivery to cancer cells. *Nanomed Nanotechnol Biol Med* 6:153–160. <https://doi.org/10.1016/j.nano.2009.05.009>
43. Vichai V, Kirtikara K (2006) Sulforhodamine B calorimetric assay for cytotoxicity screening. *Nat Protoc*. <https://doi.org/10.1038/nprot.2006.179>
44. Hsiao PH, Anbazhagan R, Hsiao-Ying C, Vadivelmurugan A, Tsai HC (2017) Thermoresponsive polyamic acid-conjugated gold nanocarrier for enhanced light-triggered 5-fluorouracil release. *RSC Adv* 7:8357–8365. <https://doi.org/10.1039/C6RA27563J>
45. Kok C, Hua S, Pan H, Lin J, Yang J (2008) Citric acid functionalized carbon materials for fuel cell applications. *J Power Sources* 176:70–75. <https://doi.org/10.1016/j.jpowsour.2007.10.049>
46. Rahman MJ, Mieno T (2014) Water-dispersible multiwalled carbon nanotubes obtained from citric-acid-assisted oxygen plasma functionalization. *J Nanomater* 508192:9. <https://doi.org/10.1155/2014/508192>
47. Chougule MA, Pawar SG, Godse PR, Mulik RN, Sen S, Patil VB (2011) Synthesis and characterization of polypyrrole (PPy) thin films. *Soft Nanoscience Letters* 1:6–10. <https://doi.org/10.4236/snll.2011.11002>
48. Chitte HK, Bhat NV, Walunj VE, Shinde GN (2011) Synthesis of polypyrrole using ferric chloride (FeCl₃) as oxidant together with some dopants for use in gas sensors. *J Sens Technol* 1:47–56. <https://doi.org/10.4236/jst.2011.12007>
49. Pisal SH, Harale NS, Bhat TS, Deshmukh HP, Patil PS (2014) Functionalized multi-walled carbon nanotubes for nitrogen sensor. *IOSR J Appl Chem* 7:49–52
50. Yaallapu MM, Jaggi M, Chauhan SC (2010) Cyclodextrin-curcumin self-assembly enhances curcumin delivery in prostate cancer cells. *Colloids Surfaces B Biointerfaces* 79:113–125. <https://doi.org/10.1016/j.colsurfb.2010.03.039>
51. Imani A, Farzi G, Ltaief A (2013) Facile synthesis and characterization of polypyrrole-multiwalled carbon nanotubes by in situ oxidative polymerization. *Int Nano Lett* 3:52
52. Ghosh A, Banerjee T, Bhandar S, Surolia S (2014) Formulation of nanotized curcumin and demonstration of its antimalarial efficacy. *Int J Nanomed* 9:5373–5387. <https://doi.org/10.2147/IJN.S62756>
53. Honary S, Zahir F (2013) Effect of zeta potential on the properties of nano—drug delivery systems—a review (Part 2). *Trop J Pharm Al Res* 12:265–273. <https://doi.org/10.4314/tjpr.v12i2.19>

Authors and Affiliations

P. Saheeda¹ · Y. M. Thasneem² · K. Sabira¹ · M. Dhaneesha³ · N. K. Sulfikkarali⁴ · S. Jayalekshmi¹

¹ Division for Research in Advanced Materials, Department of Physics, Cochin University of Science and Technology, Cochin, Kerala, India

² CSIR- Centre for Cellular and Molecular Biology, Hyderabad, India

³ National Centre for Aquatic Animal Health, Cochin University of Science and Technology, Cochin, Kerala, India

⁴ PG and Research Department of Physics, Farook College, Calicut University, Kerala, India